



Molecular Crystals and Liquid Crystals

Publication details, including instructions for authors and subscription information:

<http://www.tandfonline.com/loi/gmcl20>

Phase Transformations And Dynamics Of 4-Cyano-4'-Pentylbiphenyl (5cb) By Nuclear Magnetic Resonance, Analysis Differential Scanning Calorimetry, And Wideangle X-Ray Diffraction Analysis

T. Mansaré^a, R. Decressain^a, C. Gors^a & V. K. Dolganov^b

^a Laboratoire de Dynamique et Structures des Matériaux Moléculaires. (C.N.R.S.: U.P.R.E.S.A.8024), Université de Lille, Villeneuve d'ascq, Cedex, France

^b Institute of Solid State Physics, Russian Academy of Sciences, Chernogolova, Moscow, Russia

Version of record first published: 18 Oct 2010

To cite this article: T. Mansaré, R. Decressain, C. Gors & V. K. Dolganov (2002): Phase Transformations And Dynamics Of 4-Cyano-4'-Pentylbiphenyl (5cb) By Nuclear Magnetic Resonance, Analysis Differential Scanning Calorimetry, And Wideangle X-Ray Diffraction Analysis, *Molecular Crystals and Liquid Crystals*, 382:1, 97-111

To link to this article: <http://dx.doi.org/10.1080/713738756>

Full terms and conditions of use: <http://www.tandfonline.com/page/terms-and-conditions>

This article may be used for research, teaching, and private study purposes. Any substantial or systematic reproduction, redistribution, reselling, loan, sub-licensing, systematic supply, or distribution in any form to anyone is expressly forbidden.

The publisher does not give any warranty express or implied or make any representation that the contents will be complete or accurate or up to date. The accuracy of any instructions, formulae, and drug doses should be independently verified with primary sources. The publisher shall not be liable for any loss, actions, claims, proceedings, demand, or costs or damages whatsoever or howsoever caused arising directly or indirectly in connection with or arising out of the use of this material.

PHASE TRANSFORMATIONS AND DYNAMICS OF 4-CYANO-4'-PENTYLBIPHENYL (5CB) BY NUCLEAR MAGNETIC RESONANCE, ANALYSIS DIFFERENTIAL SCANNING CALORIMETRY, AND WIDEANGLE X-RAY DIFFRACTION ANALYSIS

T. Mansaré, R. Decressain, and C. Gors*
Laboratoire de Dynamique et Structures des Matériaux Molé-
culaires. (C.N.R.S.: U.P.R.E.S.A.8024), Université de Lille,
Villeneuve d'ascq, Cedex, France

V. K. Dolganov
Institute of Solid State Physics, Russian Academy of Sciences,
Chernogolova, Moscow, Russia

The polymorphism of 4-cyano-4'-pentylbiphenyl (5CB) was investigated by means of differential scanning calorimetry (DSC), X-ray diffraction, and proton nuclear magnetic resonance (NMR) experiments. Three new phases has been identified and characterized structurally and dynamically. By a slow cooling at a rate $\leq 0.2\text{ K/min}$, the nematic phase crystallizes into a phase noted C1. Upon a fastest cooling ($\geq 5\text{ K/min}$) a glassy liquid crystal (GLC) phase with a glass transition temperature $T_g = 208\text{ K}$, is formed. Upon heating up both the solid state C1 and the GLC phase, a second crystalline phase C2 ($\Delta H = 49\text{ J/g.K}$) which is more stable than C1 ($\Delta H = 36\text{ J/g.K}$) can be obtained. The proposed phase diagram has been investigated by proton NMR lineshape analysis. The motional correlation time of end-chain methyl group motion was determined by means of spin-lattice relaxation time (T_1) analysis.

Keywords: 5CB, dynamics, NMR, Polymorphism, X-Ray Diffraction

Received 9 April 2002; accepted 29 May 2002.

T. Mansaré thanks the Mission of Cooperation and Cultural Action of Embassy of France at Conakry for financial support.

*Present address: Laboratory of Solid State Physics/Electronic Department of Physics. University of Conakry. BP 1147. REPUBLIC OF GUINEA.

Address correspondence to R. Decressain, Laboratoire de Dynamique et Structures des Matériaux Moléculaires, C.N.R.S.: U.P.R.E.S.A.8024, université de Lille1, Villeneuve d'ascq, Cedex, France. E-mail: regis.decressain@univ-lille1.fr

INTRODUCTION

In recent years, studies of materials confined in porous media have proved to be very useful in exploring both fundamental physics of condensed matter and its industrial applications [1]. However, in the particular case of liquid crystals, the interpretation of experimental results in terms of temperature dependence is generally difficult due to the lack of an achieved polymorphism diagram. It is well-known that liquid crystals can form numerous solid modifications according to the applied thermal treatment. This structural variety is due not only to the phase transition between stable modifications but also to the possibility of obtaining metastable phases upon heating of a glassy phase. An example of such behavior is p-methoxy-benzylidene-p-n-butylaniline (MBBA), where seven phases have been identified [2].

In the present paper, X-ray diffraction and Differential Scanning Calorimetry (DSC) experiments were performed to establish the phase diagram of 5CB. Since the works of Shashidar et al. [3], Chielewski [4], Leadbetter et al. [5] and Dong [6], substantial efforts have been devoted to structural transformation, intermolecular order, and orientational molecular dynamics in the isotropic and nematic phases of liquid crystal 5CB. Up to now, little information is available from the low temperature phase transformations. In addition, proton Nuclear Magnetic Resonance (NMR) was used to characterize the phase diagram proposed by means of line-shape measurements and spin-lattice relaxation time (T_1) in the solid state and glassy liquid crystal (GLC) phase of 5CB in order to characterize molecular motions. On the basis of experimental data analysis, the correlation time and activation energy of the end-chain rotation were determined and conclusions were drawn about the relationship between molecular dynamics and phase transitions. These results are of particular interest in order to understand the behavior resulting from the confinement of 5CB in microporous materials that have been the subject of a lot of recent investigations [7 and references therein].

EXPERIMENTAL

The 5CB sample used in our experiment was purchased from Sigma Aldrich (France). A Perkin-Elmer DSC7 calorimeter was used to register the thermograms in the temperature range 173 K–323 K. The 5CB sample weight (3.32 mg) was placed in a sealed capsule. Before the measurements, the calorimeter was calibrated using materials of known phase transition temperatures.

X-ray studies were run on apparatus equipped with a curved linear position sensitive X-ray multidetector (INEL-CPS120). Monochromatiza-

tion of the incoming X-ray $\text{CuK}_{\alpha 1}$ beam ($\lambda = 1.54056 \text{ \AA}$) was performed with the (1, 0, 1, 1) Bragg reflection of a curved quartz monochromator. A more detailed description of the apparatus was made elsewhere [6]. A cryostat [8] having a temperature adjustment accuracy of 0.1 K was used in low temperature measurements. For X-ray studies the liquid-crystalline sample was introduced into a Lindeman glass capillary tube of 10 mm in length and 0.7 mm in diameter. The diffraction was measured in a plane perpendicular to the capillary axis.

The NMR experiments were carried out on a spectrometer operating at 100 MHz (ASX 100 Bruker). ^1H Zeeman spin-lattice relaxation time T_{1Z} was measured with a saturation recovery pulse sequence $[(\pi, \frac{\pi}{2}, \pi, D_0)_n]$ typically using 16–18 values of τ and recycle delay $D_0 > 5T_1$. The sample was sealed under vacuum in glass tubes and the temperature was controlled by a conventional gas flow system between 110 K and 400 K to within ± 1 K. In all cases the magnetization recovery was, within experimental errors, exponential and could be described by a single time constant.

RESULTS AND DISCUSSION

DSC Measurements

Figure 1a shows the DSC slow cooling curve of 5CB sample at a scanning rate of 0.2 K/min. Two peaks are observed: the isotropic (I)–nematic (N) transition (308 K), which is followed at lower temperature (252 K) by the crystallization of the nematic phase into a solid state. This crystallized phase will be referred to as C1. In Figure 1b the DSC curve of 5CB sample shows an exothermic peak at 257 K, obtained on heating scan at 5 K/min after cooling. We can assume that the observed crystallization is a transition of C1 phase towards solid state Cx (C1–Cx transition), which melts at 295 K (crystalline phase (Cx)–N transition). At higher temperature (308 K), the clearing N–I transformation is observed. The melting temperature (Cx–N) and the clearing transition temperature (N–I), are in accord with the DSC and X-ray results reported in the previous publications [3,4].

The DSC cooling and heating curves of 5CB sample at scanning rate of 5 K/min are presented in Figure 2. The DSC cooling scan curve (Figure 2a) shows a unique exothermic peak at 308 K, corresponding to the I–N transition. The nematic phase of 5CB can be easily supercooled. A GLC can be obtained at slow cooling rate; even at 1 K/min the 5CB sample can be quenched partially, which is much lower than for MBBA (40 K/min) [2]. In Figure 2b, the heat capacity curve presents a typical anomaly for the transition from a GLC (the glassy temperature $T_g = 208 \text{ K}$ was defined as the inflection point on the DSC heating curve). The exothermic peak observed at 239 K after the GLC was heated above the glassy transition

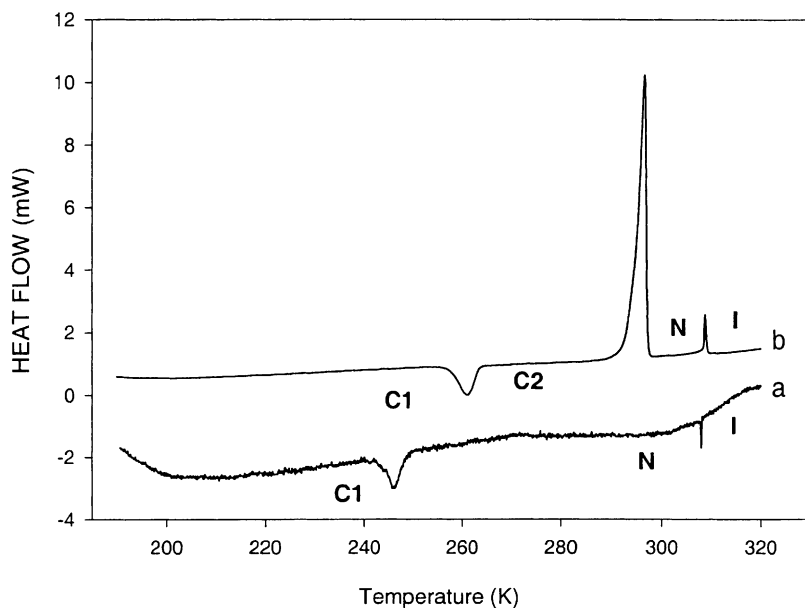


FIGURE 1 DSC slow cooling curve of 5CB sample (a) at a scanning rate of 0.2 K/min (b) DSC heating scan curve at 5 K/min.

corresponding to the crystallization into a crystalline phase, which we have noted C2 (GLC–C2 transition). On heating the endothermic peaks associated with the solid state (C2)–N transition and N–I transition are observed clearly at 295 K and 308 K, respectively. The transition enthalpies extracted from the DSC curves obtained by integration over the transition peaks are given in Table 1.

According to the melting temperature and the transition enthalpy (respectively 295 K and 67 J/g.K) measured in both heating treatments ($C_x \rightarrow N$ and $C2 \rightarrow N$ transitions), we can assume that the crystallization observed through the previous thermal treatment (Figure 1b), is a transformation into C2 ($C_x = C2$). Therefore the phase C2 can be obtained by heating the GLC or by heating C1. The transformation enthalpy of C2 exceeds that of C1, which shows that C2 is a more stable phase than C1.

X-Ray Measurements

Figure 3 illustrates the results of X-ray measurements of 5CB. All the notations of phase are consistent with those adopted in DSC experiments. The X-ray curve (Figure 3a) of the N phase is characterized by the diffuse

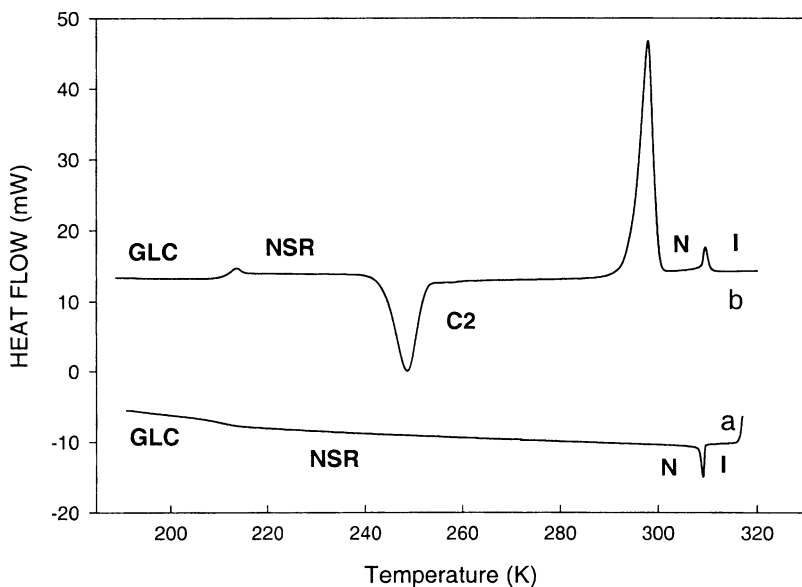


FIGURE 2 DSC (a) cooling and (b) heating curves of 5CB sample at scanning rate of 5 K/min.

and broad peak of the “liquid ring.” In X-ray diffraction the slow cooling of 5CB at a rate of 0.2 K/min from the nematic phase leads at 252 K to the formation of C1 (Figure 3–b). Three small peaks at low value, viz, $Q=0.6 \text{ \AA}^{-1}$ are observed and several peaks appear at the liquid ring position. On continuous slow cooling down to 150 K, we did not observe any modification of the X-ray pattern and no other transition was detected.

TABLE 1 Phase Transition Temperatures And Enthalpies Extracted From the DSC Curves of 5CB Sample in the both cases of Thermal Treatment (The Slow Cooling at a Scanning Rate of 0.2 K/min, Followed the Heating at a Scanning Rate of 5 K/min and the Cooling and Heating at a Scanning Rate of 5 K/min of 5CB)

Phase Transition	Transition Temperature T(K)	Enthalpies Transition ($\Delta H/\text{Jg}^{-1}\text{K}^{-1}$)
I \rightarrow N	308	2.00
N \rightarrow C1	252	36.00
C1 \rightarrow Cx	257	13.00
Cx \rightarrow N	295	67.00
GLC	$T_g = 208$	1.00
GLC \rightarrow C2	239	49.00
C2 \rightarrow N	295	67.00
N \rightarrow I	308	2.00

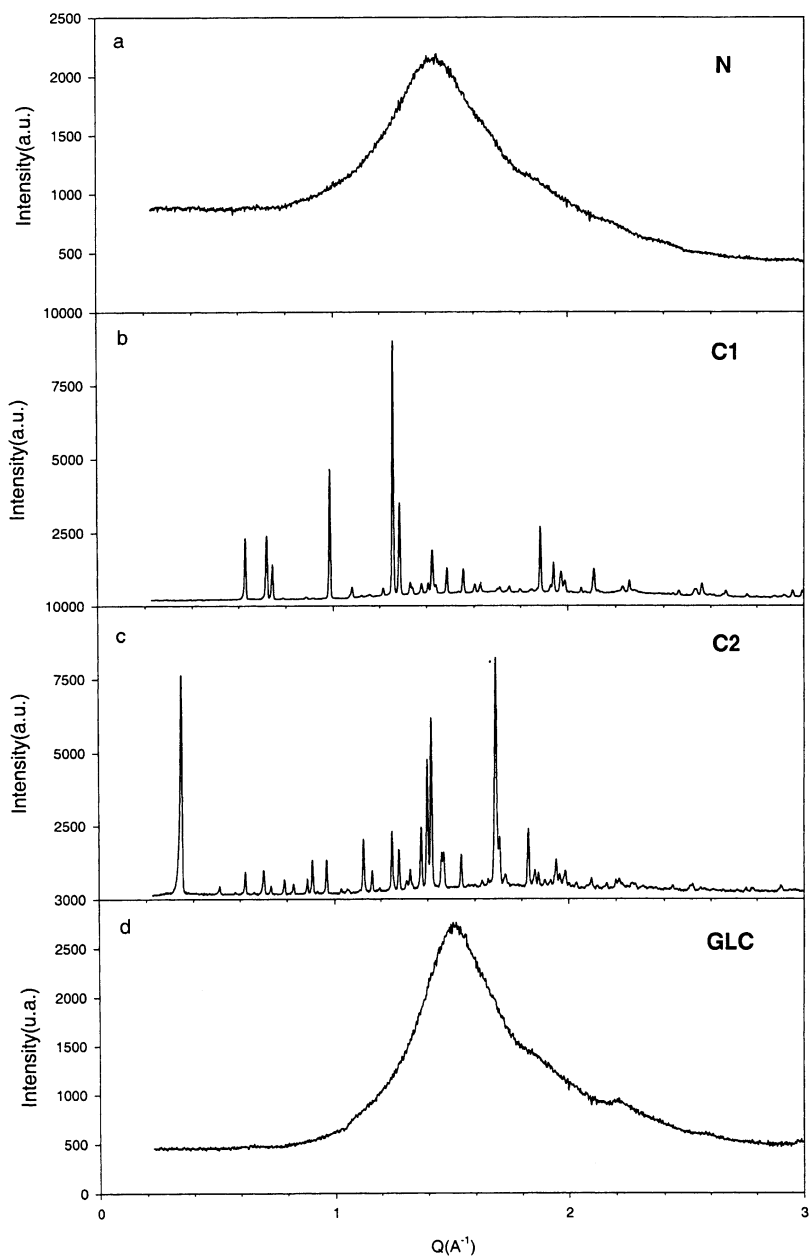


FIGURE 3 X-ray diffraction patterns of 5CB in (a) N, (b) C1, (c) Solid state C2, and (d) GLC.

By heating at a rate of 5 K/min, after cooling the X-ray curve changes (Figure 3c) at 255 K. Now, one order of intense Bragg peak is visible at low value, viz $Q = 0.3 \text{ \AA}^{-1}$, and numerous intense peaks are observed at the liquid ring position. On continuous heating, the Bragg peaks disappear and the melting is observed at 295 K. According to the DSC notations, this crystallized phase is called C2.

The quench of 5CB sample from the nematic phase leads to a phase whose X-ray pattern (Figure 3d) is similar to the N phases X-ray pattern. The width of the peak decreases in this state. Both the X-ray curve of the N and the quenched GLC can be fitted with three broad Lorentzian. The higher peak in the liquid ring, at $Q = 1.43 \text{ \AA}^{-1}$ (N) and $Q = 1.51 \text{ \AA}^{-1}$ (GLC), corresponds to a mean intermolecular distance between the long molecular axis of 4.16 \AA (160 K, GLC) and 4.39 \AA (295 K, N). The full width at half maximum (FWHM) narrows from 0.57 \AA^{-1} in the nematic phase to 0.40 \AA^{-1} in the GLC, which means that the transverse correlation extends over a longer distance.

Figure 4 illustrates the temperature dependence of the correlation length (L_r) at cooling of the nematic phase to the glassy state. The FWHM of the higher peak characterizes the correlation length (L_r) of local molecular order, following Leadbetter et al. [5]. The size of the short-range

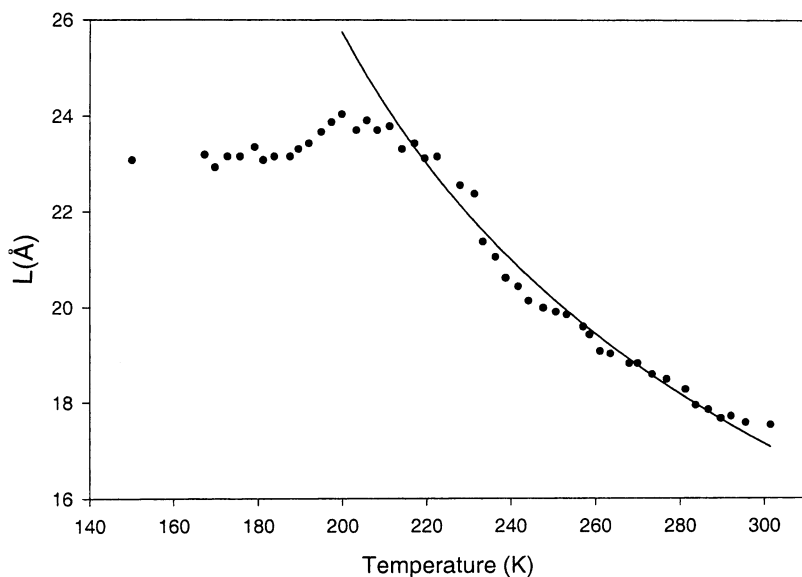


FIGURE 4 Temperature dependence of the correlation length (L_r) upon cooling of the nematic phase to the GLC phase. The continuous curve corresponds to the fit carried out with a Landau formula [10].

order region was estimated using the Hosemann's model [8,9]. The relationship between the width of the diffraction line ΔQ and correlation length L_r has the form [8,9]

$$L_r = \frac{2\pi^3}{6.25\Delta Q}. \quad (1)$$

The value of L_r in the nematic phase is in accordance with the results found by Leadbetter et al. [5]. The continuous variation in L_r was observed from the nematic phase to the glassy phase. Besides this modification no change could be detected. The structure of the GLC phase appears to be very similar to the structure of the nematic phase.

In the T_g region a small maximum of L_r can be observed (Figure 4). Solidification of the sample as it transitions to the glassy state is accompanied by a distortion of the molecular packing, which is reflected by the decrease of L_r .

By heating at 5 K/min, the GLC is followed a crystalline phase (Figure 3c). We observed one intense Bragg peak at small value of Q and numerous peaks at the liquid ring position. The crystallization of this phase is observed at 255 K. The X-ray curve is similar to the X-ray curve of the crystalline C2 phase (Figure 3c). On continuous heating, melting to the nematic phase occurs at 295 K. Therefore the phase C2 can be obtained by heating the GLC or by heating C1, as is seen in the DSC experiments.

In the isotropic phase, the correlation length ξ that characterizes the orientational molecular ordering increases when the temperature decreases. The variations of ξ are described by the power function $\xi = \xi_0(T^*/(T - T^*))^v$ with an index $v = 0.5$, following from Landau theory [10]. T^* is the temperature of the absolute instability limit of liquid with respect to transition to a phase having a long-range orientational order. ξ_0 is a molecular length. However, at cooling the overall correlation length L_r that characterizes the translational and orientational ordering also increases. Like in the case of the orientational ordering, one can attempt to describe a variation of L_r by the power function

$$L_r = L_0 \left(\frac{T^*}{T - T^*} \right)^{0.5}. \quad (2)$$

The curve in the Figure 4 conforms to $T^* = 120$ K, $L_0 = 21$ Å. In our case, T^* corresponds to an infinite value of L_r , that is to say, to a structure having a molecular long-range order analogous to the liquid crystalline local ordering. The difference $T_g - T^*$ amounts to 102 K, which is much in excess of the value obtained for the I-N transition (#1K). This is due to the fact that the transition with translational and orientational order is stronger first-order transition compared to the I-N transition.

On cooling the nematic phase, T^* was not achieved since at higher temperature, ($T_g > T^*$), the viscosity increases and the material changes to the glassy state. The question remains open whether in principle T^* could be achieved upon rapid cooling if, prior to this, no crystallization or transition to glassy state occurs. This might be possible in the case when short-range molecular order is compatible with macroscopic three-dimensional ordering.

NMR ^1H Measurements

In the NMR experiments, the sample was first heated up to 330 K, corresponding to the isotropic state, and afterwards was slowly cooled down into the nematic phase (295 K). The measurements were then performed as a function of temperature by two different procedures. The 5CB sample was first slowly cooled from the nematic phase. Slow cooling was accomplished by lowering the temperature in 5 K intervals, waiting 10 min for the sample to come to thermal equilibrium. In the second method, the sample was quenched from the nematic state at maximum speed rate in order to reach the GLC state. Measurements were then performed at increasing temperature from 110 K to 210 K. The solid phase C2 was obtained after an annealing of several hours at 225 K of the GLC phase.

Line Shape Analysis

First we have used proton NMR line-shape analysis in order to characterize by NMR the low temperature phases of 5CB. Starting from the isotropic phase a complete assignation of the proton spectrum was done and the purity of the sample was checked. Figure 5 shows the ^1H NMR spectra recorded upon a slow cooling. The NMR spectra of the nematic phase is clearly identified by the appearance of the classical double doublets, arising respectively from the end-chain and phenyl protons [6,10]. At 300 K the separation of those doublets is respectively 9.5 KHz and 21.5 KHz; whereas at 230 K just before the crystallization to C1, the variation of the orientational order parameter resulted in an increase of these values to 17.1 KHz and 28.5 KHz. According to the proton lineshape evolution, the $\text{N} \rightarrow \text{C1}$ phase transition is observed between 255 and 250 K, which corresponds to the temperature previously determined by DSC. In the solid phases, due to the increase of the dipolar coupling, a single broad line without any structural particularity is observed. However, as a more important line-width is observed upon reheating the glassy state than upon a slow cooling experiment (36.4 KHz and 34.4 KHz respectively at 200 K), our NMR line-shape investigation confirms both the existence of a glassy liquid crystal GLC, and two solid phases (C1 and C2) where the effective motional narrowing is different. On the other hand, as previously observed in the

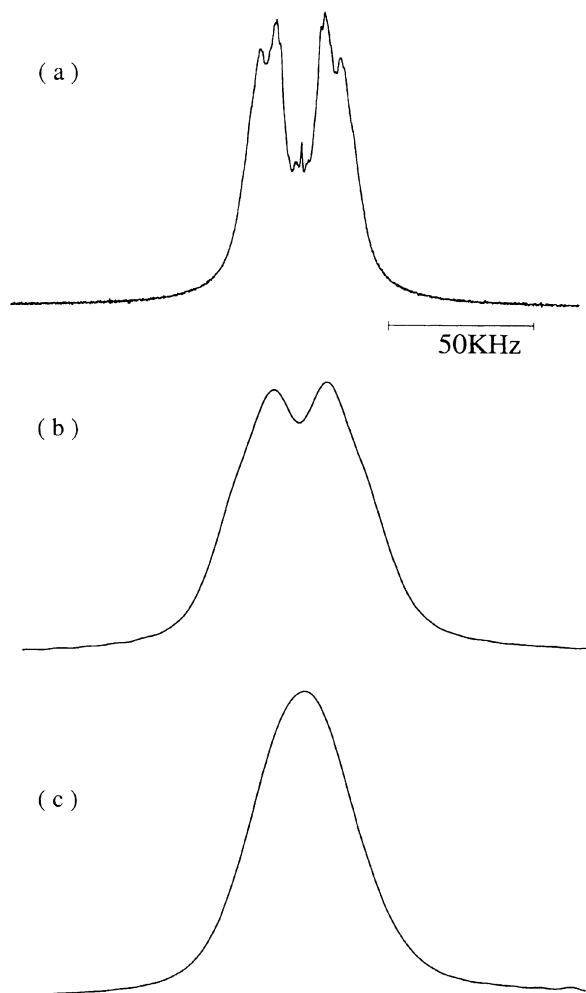


FIGURE 5 Typical ^1H NMR line shapes of bulk 5CB in the (a) nematic, (b) GLC, (c) Solid state C1.

nematic phase, the NMR spectrum of a quenched sample is composed of a doublet ($\cong 19$ KHz at 200 K), indicating that an amount of orientational order is still present in the glassy state.

Spin-Lattice Relaxation Times Analysis

The temperature dependence of the proton spin-lattice relaxation time T_1 is represented in Figure 6. Upon a slow cooling the general behavior of the

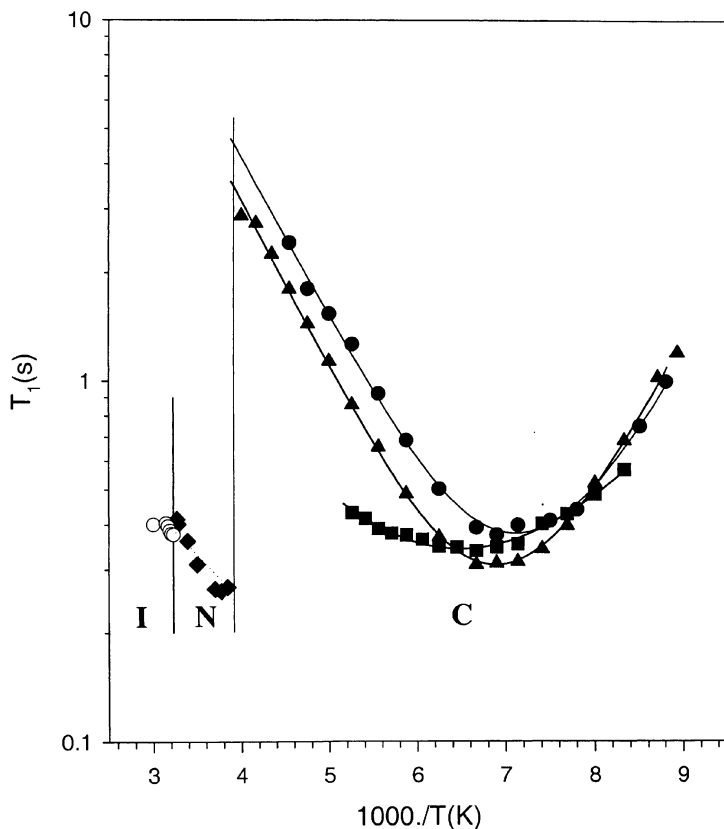


FIGURE 6 Variation of ^1H T_{1z} versus $10^3/T(\text{K})$ at 100 MHz for (○) Isotropic, (◆) nematic, (■) GLC, (●) Solid state C2, and (▲) Solid state C1. The continuous curves correspond to the refinement carried out with a rotational isotropic diffusion (BPP) model. (13).

temperature dependence of T_1 is connected with the phase transitions observed by other techniques. The crystallization to the solid phase C1 results in an important increase of T_1 , from 0.25 to 3 s at 252 K, which is in good agreement with lineshape analysis. As the temperature is decreased, a minimum is observed in C1 at 147 K with $T_1 \approx 305$ ms. The GLC state, as generally observed for glassy materials [11], is characterized by a rather small variation of T_1 , which lies between 0.32 and 0.45 s between 200 K and 120 K. Upon heating a quenched sample at 200 K, T_1 increases abruptly to 2.3 s at 230 K. As this value is substantially more important than those obtained for C1 at the same temperature, a GLC-C2 phase transition is perceived by NMR relaxation time analysis.

Because a symmetric V shape of the T_1 data versus inverse temperature is observed, we have assumed (as it has been previously shown in other similar compounds) that the spin lattice relaxation rate is governed by the CH_3 reorientation around its C_3 axis. In this case, if we assumed that all other protons in the solid are relaxed by rapid spin exchange to and from the methyl group, the temperature dependence of T_1 is given by the well-known BPP expression [13].

$$\frac{1}{T_1} = C_{\text{BPP}} g(\omega, \tau_m), \quad (3)$$

and with Andrew and Peplinska [14]:

$$C_{\text{BPP}} = \frac{9}{20} \frac{n}{N} \left(\frac{\mu_0}{4\pi} \right)^2 \frac{\gamma^4 \hbar^2}{r_m^6}, \quad (4)$$

where N is the number of protons in the molecule and n is the number of protons in the methyl group contributing to the relaxation process. The distance r_m is the inter-proton distance in the methyl group. By assuming $r_m = 1.80 \text{ \AA}$, the parameter C_{BPP} can be interpreted as the strength of the spin-lattice coupling due to the intra-methyl proton dipole-dipole interactions, diluted by n/N , which is the ratio of the number of protons involved in the motion to the number of protons in the molecule. For 5CB, we have performed a numerical evaluation of C_{BPP} using $n = 3$ and $N = 19$. If dipole-dipole interactions between methyl protons and other protons are important, C_{exp} will be larger than C_{BPP} in Equation (4), but C_{BPP} gives a lower limit indicative of the type of motion involved in the relaxation process.

The function g in Equation (3) is given by Andrew and Peplinska [14]:

$$g(\omega, \tau_i) = \frac{\tau_i}{1 + \omega^2 \tau_i^2} + \frac{4\tau_i}{1 + 4\omega^2 \tau_i^2}, \quad (5)$$

where $\omega = \gamma H$. H_0 is the Larmor frequency, and correlation time τ_i is related to the temperature via an Arrhenius relationship,

$$\tau_i = \tau_{\infty i} e^{\frac{E_i}{RT}}, \quad (6)$$

which introduces the activation energy E_i and the pre-exponential factor $\tau_{\infty i}$.

The fit of the data are represented by solid lines in Figure 6, and the correlation times are displayed in Figure 7. In all phases the experimental data are well fitted by this model and the motional parameters listed in Table 2.

The deviation from unity of the ratio $C^{\text{Fitted}}/C^{\text{BPP}}$ is very small in GLC and C2. This results show that it is sufficient to take into account only intra-methyl proton-proton interactions and that the origin of relaxation is mainly

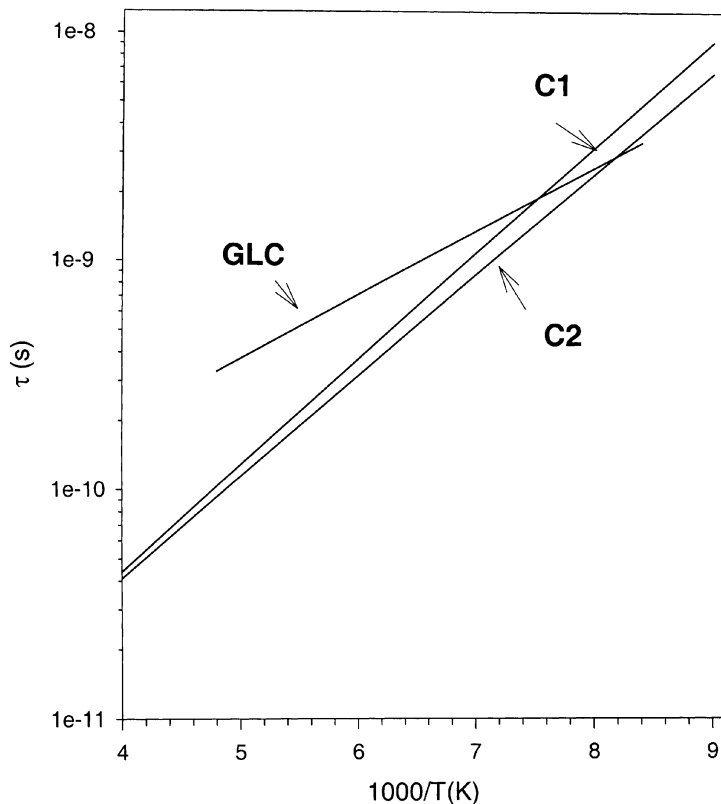


FIGURE 7 The mean residence times τ versus $1000/T(K)$ obtained in the GLC C1 and C2 phases of 5CB by 1H NMR analysis.

due to the C_3 axis reorientation of the methyl groups. This implies that, contrary to some other examples of liquid crystals solid phases, the C_3 axis probably remains fixed in the lattice. In solid state C2, a decrease of this ratio suggests a more important influence of the intermolecular interactions, probably related to a different steric hindrance of the molecules.

TABLE 2 Parameters of the Relaxation Model, Evaluated from the T_1 Temperature Dependence in the Solid Phases of 5CB

Phase	$C^{\text{fitted}}/C^{\text{BPP}}$	τ_0 (s)	E_a (KJ/mol)
GLC	0.92	$(0.15 \pm 0.01)10^{-10}$	5.3 ± 0.8
C1	0.83	$(0.61 \pm 0.04)10^{-12}$	8.9 ± 0.8
C2	0.98	$(0.69 \pm 0.02)10^{-12}$	8.5 ± 0.3

The barriers for methyl reorientation are in the range 5.3 to 8.9 KJ/mol. The E_a values are approximately the same respectively in C1–C2, where the smallest activation energy was obtained for GLC phase. Similar behavior has already been reported for relaxation in the glassy and solid phases of MBBA [11,12]. The small barrier measured in GLC confirms—in good agreement with the line-shape analysis—that the local arrangement of the nematic state is globally conserved on quenching the sample. As E_a increases in C1 and C2, the crystallization induced an increase of the steric hindrance of the molecules, which prevents ethyl group reorientations from occurring in these phases as it has been observed in MBBA and p-ethoxy-benzilidene-p-n-butylaniline (EBBA) [11, 15].

CONCLUSION

A preliminary investigation has been made of the polymorphism and molecular dynamics of 5CB. More efforts have to be made in this direction for a complete understanding of the phase diagram, the influence of the thermal treatment on GLC state formation, and the relationship between the rotational dynamics and the various phase transitions of 5CB. The nematogen 5CB is a good example of a glass forming liquid crystal. In particular, 5CB possesses the advantage of being very easily quenched when starting from the nematic phase. The quenched phase GLC is very similar to the nematic phase, exhibiting a better transverse short-range order. However, the phase diagram of 5CB is not yet as well known as those of MBBA, for example. In this work we have shown the existence of a GLC phase and of a metastable crystalline phase C1 obtained by slow cooling of 5CB sample. A stable crystalline phase C2 can be obtained by heating of the GLC or by heating of the metastable solid state C1. The motional parameters of methyl group motion are obtained from ^1H NMR analysis in each solid phase.

REFERENCES

- [1] L. D. Gelb, K. E. Gubbins, R. Radhakrishnan, and M. Sliwinska-Bartkowiak, *Rep. Prog. Phys.*, **62**, 1 (1999).
- [2] G. Peppy, R. Fouret, M. More, and L. Rosta, *Liq. Crystals*, **5**, 571 (1989).
- [3] R. Shashidar and G. Venkatesh, *J. of Phys.*, Coll. **C3 40**, (Suppl.), C3–396 (1979).
- [4] A. G. Chielewski, *Mol. Cryst. Liq. Cryst.*, **132**, 303 (1986).
- [5] A. J. Leadbetter, R. M. Richardson, and C. N. Colling, *J. of Phys.*, Coll. **C1 36**, (Suppl.) C1–37 (1975).
- [6] R. Y. Dong, *NMR of Liquid Crystals*, (Springer-Verlag, New York, 1994).
- [7] G. S. Iannachione, S. Qian, D. Finotello, and F. M. Aliev, *Phys. Rev. E*, **56**, 554 (1997).
- [8] G. Odou and D. Naviez, *Spectra 2000*, **17** (1987).

- [9] B. K. Vainshtein, *Diffraction of X-ray by Chain Molecules* (Elsevier, Amsterdam, 1966).
- [10] P. G. De Gennes and J. Prost, *The Physics of Liquid Crystals* (Clarendon Press, Oxford, 1993), 2nd ed., Chap. 2, p.82.
- [11] R. Decressain, E. Cochin, T. Mansare, and M. More, *Liq. Crystals*, **25**, 517 (1998).
- [12] V. K. Dolganov, I. Pòcsik, and L. Rosta, *Liq. Crystals*, **14**, 1895 (1993).
- [13] N. Bloembergen, E. M. Purcell, and R. V. Pound, *Phys. Rev.*, **73**, 679 (1948).
- [14] E. R. Andrew and B. Peplinska, *Mol. Phys.*, **70**, 505 (1990).
- [15] M. Froix and J. Yanus, *Mol. Cryst. Liq. Cryst.*, **51**, 167 (1979).